# Recognition of a porphyry system using ASTER data in Bideghan - Qom province (central of Iran)

**F. Feizi[1] and E. Mansouri[2]**

[1]{Department of Mining Engineering, South Tehran Branch, Islamic Azad University, Tehran, Iran}

[2]{Young Researchers and Elite Club, South Tehran Branch, Islamic Azad University, Tehran, Iran}

Correspondence to: F. Feizi(feizi.faranak@yahoo.com)

## Abstract

The Bideghan area is located south of the Qom province (central of Iran). The most impressive geological features in the studied area are the Eocene sequences which are intruded by volcanic rocks with basic compositions. Advanced Space borne Thermal Emission and Reflection Radiometer (ASTER) image processing have been used for hydrothermal alteration mapping and lineaments identification in the investigated area. In this research false color composite, band ratio, Principal Component Analysis (PCA), Least Square Fit (LS-Fit) and Spectral Angel Mapping (SAM) techniques were applied on ASTER data and argillic, phyllic, Iron oxide and propylitic alteration zones were separated. Lineaments were identified by aid of false color composite, high pass filters and hill-shade DEM techniques. The results of this study demonstrate the usefulness of remote sensing method and ASTER multi-spectral data for alteration and lineament mapping. Finally, the results were confirmed by field investigation.

**Keywords:** ASTER, Bideghan , Alteration, Lineament, Porphyry, Eocene.

## 1 Introduction

Iran is located in the Alpine-Himalayan orogenic belt and Uromieh – Dokhtarmetalogenic belt is the most impotant zone in Iran which has high potentials for gold and copper as well as other base metal deposits. In Iran, satellite data such as TM, ETM+ and ASTER (Advanced

Spaceborne Thermal Emission and Reflection Radiometer) have been used by geologists for exploration purposes (AsadiHaroni and Lavafan, 2007; Azizi et al. 2010).

Intermediate to acidic igneous rocks from the late Cretaceous to Tertiary in the western ,northwestern and northern parts of Iran are important because the high value presence of copper and gold mineralization in these host rocks .These rocks have been found in the 1:100000 Kahak sheet .The studied area is located in this geological map as a part of Uromieh – Dokhtar belt. Therefore, high resolution remote sensing data and Geographic Information Systems (GIS) are important tools to map subtle anomalies associated with unknown gold and base metal deposits (Kujjo, 2010; Bell, 2011; Albanese, 2011).

Because the alteration zones recognition are the most important keys for base metal deposit exploration therefore using of methods such as remote sensing which help to separate these zones will be useful.

In this research, a spectral analysis was carried out on the ASTER satellite imagery data of the investigated area to map spectral signatures associated with the hydrothermal alterations. Least Square Fit (LS-Fit), Principal Components Analysis and band ratio methods were also performed to achieve better accuracy along with spectral analysis. In addition, lineaments by using of False Colour Composite (FCC) images, high pass filters and hill-shade DEM techniques were extracted.

Finally the integration of alteration, lineaments and litho logical features can show the hopeful areas for exploration.

There are a lot of researches in different case studies with these methods which have very good results, for example remote sensing studies in 1:100000 Soltanieh map (Feizi et al. 2013) and Iron prospecting in 1:100000 Sfordi sheet (Sadeghi et al. 2013).

## 2 Materials and methods

### 2.1 Geology setting

The studied area is located between 50˚ 56', 50˚ 59' longitude and 34˚ 17', 34˚ 20' latitude in the south of the Qom province (Northeast of 1:100000 KAHAK Sheet). Based on 1:100000 geological map of Qom, the most impressive lithological features in the studied area are the volcanic rocks with basic combinations. These features are included; Andesite, Andesibasalt and mega porphytite andesite. There are tuffaceous sandstone and lime stones in the east and southeast of the investigated area. Hematitation, limonitation, silisitaion and

argillic alterations are seen in central parts that have been formed in north-south trend in the east and northeast of the studied area. Volcanic rocks have specific conditions. For example, ferrous ore such as Oligist formed along fractures in a tectonic environment. (Agha Nabati ,2004). Based on 1:100000 geological map of Kahak, three NE-SW faults have been seen. According to study results conducted around the faults, alteration and ferrous fluid have been observed (Figure 1).

## 2.2 ASTER data

The ASTER sensor is one of the multi-spectral sensors that has been installed on the TERRA satellite.This sensor can measure the reflection of the Earth's ground in three bands, that is, between the wavelengths of 0.52–0.86 l m with a resolution of 15 m (visible and near-infrared: VNIR), six bands between the wavelengths of 1.6–2.43 lm with a resolution of 30 m (SWIR), and five bands between the wavelengths of 8.125–11.65 lm with a resolution of 90 m (thermal infrared: TIR) (Figure 2). (Rowan & Mars, 2003; Moghtaderi et al., 2007; Yousefifar et al., 2011).Furthermore, the TERRA satellite has a back-looking telescope with a resolution of 15 m in the VNIR that matches with the wavelength of the band 3 that is used to extract 3D information. Meanwhile, the sensor swath of ASTER is 60 km (Yamaguchi et al., 2001; Rowan et al., 2006). According to extreme variations of spectral reflectance curves of minerals in the SWIR region and high spectral resolution of the ASTER sensor, the sensor identifies different rocks and minerals on the Earth's surface effectively. Considering the differences of the sensor resolution capability between $ETM^+$ and ASTER sensors, usually $ETM^+$ images are used for the lineaments and ASTER images are used to identify minerals and alterations of the Earth's surface. The ASTER is an advanced optical sensor comprised of 14 spectral channels ranging from the visible to thermal infrared region. It will provide scientific and also practical data regarding various field related studies of the earth (Watanabe and Matsuo, 2003). Various factors affect the signal measured at the sensor such as the drift of the sensor radiometric calibration, atmospheric and topographical effects. For accurate analysis, all of these corrections are necessary for remote sensing imagery. To this end, at the beginning of the path, data set in hierarchical data format (HDF) was used for this research and radiance correction such as wavelength, dark subtract and log residual by ENVI4.4 software which was essential for multispectral images were implemented. ASTER bands have good sensitivity for alteration minerals. For example VNIR band is good for Iron oxide and SWIR is good for argillic alteration in band 4,propellitic alteration in band 6 and

phyllicalteration in band 4, 5 or 8 usually. Also TIR include thermal bands for silica identification usually.

## 3 Result and discussion

### 3.1 Hydrothermal Alteration Detection

Many image analysis and processing techniques can be used to interpret the remote sensing spectral data. In this research, False Color Composite (FCC), Minimum Noise Fraction (MNF), Principal Component Analysis (PCA), Least Square Fit (LS-Fit) and Spectral Angle Mapping (SAM) methods were used on the ASTER data for the discrimination of alteration zones.

#### 3.1.1 False color composite (FCC)

The studies on re-sampling of USGS standard curves on ASTER bands show that Al-OH minerals such as kaolinite, muscovite, montmorilonite and illite (major minerals for phyllic and argillic alteration zones) have the most reflection in B4 on SWIR (Figure 3). Also, Mg-OH minerals such as chlorite and epidote that are remarkable for propylitic alteration zones have the most reflection in Band 5 and 6 on SWIR. (Yetkin et al. 2004. Figure 4)

Therefore, phyllic and argillic alteration zones are shown reddish to pink and propylitic alteration zones are shown green in 468 False Color Composite (FCC) on SWIR. (Beiranvnd Pour et al. 2011). (Figure 5)

#### 3.1.2 Principal Component Analysis

The Principal Component Analysis (PCA) is a multivariate statistical technique that selects uncorrelated linear combinations (eigenvector loadings) of variables. Each successively extracted linear combination, or principal component (PC), has a smaller variance. The PCA is widely used for alteration mapping in metallogenic provinces (Myint, et al., 2005) and has been applied in this study. An approach based on the examination of eigenvector loadings in each PC image is used for determining which image contains information related to the spectral signatures of specific target minerals. It is expected that the PC image that collects moderate to high eigenvector loadings for the diagnostic absorptive and reflective bands of the index mineral could be considered as the specific image for that mineral. If the loading of the absorptive band is negative in sign the target area will be enhanced in bright pixels, and if the loading of the reflective band is negative the area will be enhanced in dark pixels (Crosta and Moore, 1989; Khaleghi, and Ranjbar, 2011).

Table 1 shows the eigenvector loadings for bands 1, 2, 3 and 4. In this table at a $\frac{2}{1}$ ratio and at a $\frac{3}{1}$ ratio should not be + or – both. These ratios must be $\frac{+}{-}$ (normal case) or $\frac{-}{+}$ (Inverse case). Inverse case has to correct. The analyses which have done on table 1 show in PC3,$\frac{3}{4}$ ratio is $\frac{-}{+}$ so it should study in inverse case. In PC4 $\frac{2}{1}$ ratio is $\frac{-}{+}$ and $\frac{3}{4}$ ratio is $\frac{+}{-}$ so PC4 have to study in both case. Base on this investigation PC3 shows good results in inverse case. Inverse of PC3 can show the areas with iron oxide. Table 2 shows the eigenvector loadings for bands 1, 4, 5 and 7. In PC1,$\frac{5}{7}$ ratio is $\frac{+}{-}$ so it should study in normal case. In PC2 $\frac{4}{1}$ , $\frac{5}{7}$ ratios are $\frac{+}{-}$ so they should study in normal case . In PC3,$\frac{4}{1}$ ratio is $\frac{+}{-}$ so it should study in normal case. In PC4 $\frac{4}{1}$ , $\frac{5}{7}$ ratios are $\frac{-}{+}$ so they should study in inverse case. Base on this investigation PC3 shows good results in normal case. According to the results, the image related to PC3 shows the argillic alteration. Table 3 shows the eigenvector loadings for bands 1, 3, 5 and 6. In PC2,$\frac{3}{1}$ ratio is $\frac{-}{+}$ so it should study in inverse case and In PC3,$\frac{3}{1}$ and $\frac{5}{6}$ratios are$\frac{+}{-}$ so they should study in normal case. In PC4,$\frac{3}{1}$ratio is $\frac{-}{+}$ so it should study in inverse case. Base on this investigation PC4 shows good results in inverse case. Inverse of PC4 can show the areas with phyllic alteration. Table 4 shows the eigenvector loadings for bands 2, 5, 8 and 9. In PC2,$\frac{5}{2}$ ratio is $\frac{+}{-}$ so it should study in normal case. In PC3,$\frac{5}{2}$ , $\frac{8}{9}$ ratios are$\frac{+}{-}$ so they should study in normal case. In PC4,$\frac{5}{2}$ ratio is $\frac{+}{-}$ so it should study in normal case. Base on this investigation PC4 shows good results in normal case. PC4 can show the areas with propylitic alteration (Figure 6).

### 3.1.3 Least Squares Fitting (LS-Fit)

The technique assumes that the bands used as input values are behaving as the variables of a linear expression and the 'y' value of the equation, namely the predicted band information, gives us a calculated output value. This predicted band is what the band should be according to the linear equation. The minerals which are sensitive to a specific band are then differentiated from the features which are reflective to the other bands as well by simply taking the difference between the predicted values and the original values (Yetkin et al. 2004).

Distribution of iron oxide was created by using all three visible and near-infrared (VNIR) bands as the input bands and VNIR-b1 as the modeled band. Also, argillic, phyllic and

propylitic alterations were mapped by using residual band SWIR-b1, residual band SWIR-b3 and residual SWIR-b6 (Figure 7).

### 3.1.4 Minimum Noise Fraction (MNF)

The Minimum Noise Fraction (MNF) transformation was used to determine the inherent dimensionality of image data, segregate noise in the data and reduce the computational requirements for subsequent processing (Boardman et al. 1995; Green et al. 1988; Beiranvnd Pour et al. 2011).PCA is a method for decreasing repetitive data and nuisance features as shades, topographical effects and sun radiation angel. This method is based on standard deviation, variance and covariance calculations. MNF like PCA is good for decreasing later calculations. In his research, both methods were used for controlling the results with comparing them. MNF involves two steps. In the first step, which is also called noise whitening, principal components for noise covariance matrix are calculated. This step decorrelates and rescales the noise in the data. In the second step, principal components are derived from the noise whitened data. The data can then be divided into two parts. One part associated with large Eigen values and the other part with near unity Eigen values and noise dominated images. Using data with large Eigen values separates the noise from the data, and improves spectral results (Green et al. 1988; Beiranvnd Pour et al. 2011). MNF analysis can identify the locations of spectral signature anomalies. This process is of interest to exploration geologist because spectral anomalies are often indicative of alterations due to hydrothermal mineralization (Beiranvnd Pour et al. 2011). MNF bands 2, 6, 4 (inverse) and 5 were used for iron oxide, argillic, phyllic and propylitic alterations (Figure 8).

The cause of using these methods is very good results in determination of alteration zones with these bands combination. For example in a case study in the north of this region (Feizi et al. 2012)

### 3.1.5 Spectral Angle Mapper

The Spectral Angle Mapper (SAM) is a classification technique that permits rapid mapping by calculating the spectral similarity between the image spectrums and reference reflectance spectra. SAM measures the spectral similarity by calculating the angle between the two spectra and treating them as vectors in n-dimensional space (Kruse et al. 1993), (Beiranvnd et al. 2011). The image spectra were compared with USGS Digital Spectral Library (Minerals) (Malekzadeh et al. 2009). Figure 8 shows selected minerals spectral library plots that related to argillic, phyllic and propylitic alterations. Three mineral spectral representatives of the

argillic zone include kaolinite, dickite and halloysite. Two minerals spectral representatives of the phyllic alteration consist of illite, muscovite, and epidote. Chlorite representative of propylitic zone were selected (Figure9, 10).

## 4 Lineament extraction

Lineament extraction in this study was carried out by manual method. In manual extraction method, the lineaments are extracted from a satellite image by using visual interpretation. In this research Shaded relief method and median filter were used for fault identification with using DEM image which was prepared by Geological survey of Iran. The lineaments usually appear as straight lines or “edges” on the satellite images which in all cases were contributed to the tonal differences within the surface material. The knowledge and the experience of the user is the key point in the identification of the lineaments particularly to connect broken segments into a longer lineament (Sarp, 2005).

False color images are produced for manual lineament extraction because they increase the interpretability of the data. Different combinations of three bands are examined and the best visual quality is obtained with a false color image utilizing three 7, 4, and 2 (in blue, green and red respectively). This false color combination made it easier to identify linear patterns of vegetation, geologic formation boundaries, river channels and geological weakness zones. Moreover, filtering operations are used to emphasize or deemphasize spatial frequency in the image. The filtering operation will sharpen the boundary that exists between adjacent units. Furthermore, standard GIS techniques have been carried out to help in the evaluation of the lineaments detected. Digital Elevation Model (DEM) has the advantage of representing the vertical extension of the earth's surface by assigning height values for every pixel (Papadaki et al. 2011). The Hill-shade DEM technique is also effective in creating images that enhance geomorphologic features (Weldemariam, 2009). Therefore, Hill-shades DEM with different azimuth direction and sun angle were used in this study (Figure11).

## 5 Integration of alteration and Lineament

In this part for integration the data layers in GIS area, first of all, the shape files of all alteration zones which were carried out with different methods were drown. Then the layers were overlapped on each other. Afterwards the most overlapped zones were chosen and were controlled with field investigations. As the last step, the lineament map of studied area was integrated with the final alteration map in GIS area. (Figure 12). As the figure shows, there is a very good adaptation between these two layers, especially in the east and a band with a NW-

SE trend in the south of the area. There is also a good adaptation in north of the area .Therefore, a circular band that begins from the northwest corner to the east, southeast and to the west has been recognized.

## 6 Field investigations and alteration zones control

After all these software analyses, field investigations were necessary. Figure 13 shows a full view of studied area. The control points were detected, and after the field studies, the correction of alteration zones were confirmed. Figure 14 shows the three check points for Iron oxide which were recognized with using remote sensing processes. These checking have confirmed the results of the RS methods.

As Figure 15 shows, Sericitic Muscovites, Quartz and a few of Illite have been seen in the Phllic alteration zones. The check field for Argillic alteration zones were confirmed by the results of RS methods (Figure 16). Presence of Chlorite and Epidote minerals in check field processes confirmed the Propylitic alteration zones (Figure 17). The adaptation of Iron Oxide and Argillic alteration zones is a very important guide for hydrothermal mineralization deposits, especially sulfide minerals (Figure 18).

## 7 Mapping hydrothermal alteration at porphyry copper deposits

Most of the world's copper is mined from porphyry deposits which occur in a different geologic environment. Hydrothermal alteration is also common at porphyry deposits and may be recognized by the same methods that were developed in remote sensing.

### 7.1 Alteration model

According to the model of hydrothermal alteration of porphyry copper deposits that was developed by Lowell and Guilbert _1970, Phyllic zone is the most intense alteration which occurs in the core of the porphyry body and contains Quartz, Sericite and Pyrite. Other alteration zones are Argillicand Propylitic.The most characteristic minerals inArgillic zone are Quartz, kaolinite and montmorillonite. Propyliticzone containsEpidote, calcite, and chlorite. The existence of these alterations is important key for exploration of this kind of deposits, especially, with remote sensing methods.

The ore body includes disseminated grains of Chalcopyrite, Molybdenite, Pyrite and other metal Sulfides. The most of this mineralization occurs near the boundary between the Potassic and Phyllic zones.

The porphyry copper deposits have a red to brown iron-stained crust called Gossan or leached capping which can be useful for exploration. (Sabins, 1999).

### 7.2 Check fields processes

Because the porphyry system in the research area was recognized by using remote sensing methods, field studies were necessary. These operations were successful and copper minerals indexes were evident. As Figure 18 shows, the copper hydro carbonates like Malachite and Azurite covered the surface of the rocks These minerals were recognized in the central parts of propylitic and argillic rings.

## 8 Conclusion

Presence of three dominant strikes: NE – SW, N-S, NW - SE were recognized in the studied area. The result of integration between alteration and lineaments indicate a circle band that begins from the northwest corner to the east, southeast and to the west.

There is probably a porphyry system, caused by locating of the propylitic alteration zone around the argillic alteration zone, especially in the central part of the area. The overlapping between argillic alteration and iron oxide zones indicate the presence of sulfide deposits. The phyllic alteration zone exists in the middle of the band, especially where the intrusive bodies are.

## References


Aghanabati , A. ,Geology of Iran ,Geological survey of Iran ,622 pages ,2004.

Albanese, R. , Overcoming resistance to stability :A time to move; a time to pause. Archives Des Sciences Journal, 64 ,2011.

AsadiHaroni, H. and Lavafan, A. ,Integrated Analysis of ASTER and Landsat ETM Data to Map Exploration Targets in the Muteh Gold -Mining Area, IRAN, 5th International Symposium on Spatial Data Quality, Enscheda , And The Netherlands ,2007.

Azizi, H. Tarverdi M.A. and Akbarpour, A. ,Extraction of hydrothermal alterations from ASTER SWIR data from east Zanjan, northern Iran, Advances in Space Research, 46, 99–109 ,2010.

Beiranvnd Pour, A. Hashim M. and Marghany, M., Using spectral mapping techniques on short wave infrared bands of ASTER remote sensing data for alteration mineral mapping in SE Iran . International Journal of the Physical Sciences, 6(4), 917-929,2011.

Bell, E.C. ,Practical long-range planning: Case histories show how it's actually done. Archives Des Sciences Journal, 64 ,2011.

Boardman, J.W. Kruse F.A. and Green, R.O. ,Mapping target signatures via partial unmixing of AVIRIS data, Summaries, Proceedings of the Fifth JPL Airborne Earth Science Workshop, Pasadena, California, JPL Publ., 95-1, 1: 23–26 ,1995.

Feizi, F. and Mansuri, E., Separation of Alteration Zones on ASTER Data andIntegration with Drainage Geochemical Maps in Soltanieh, Northern Iran, Open Journal of Geology, 2013, 3, 134-142.

Feizi, F. and Mansuri, E., Identification of alteration zones with using ASTER data in apart of Qom province, Central Iran, Journal of Basic and Applied Scientific Research, 2(10)10173-10184, 2012.

Green, A.A. Berman, M. Switzer P.and Craig, M.D., A transformation for ordering multispectral data in terms of image quality with implications for noise removal, IEEE Tran. Geo. Rem. Sen., 26(1): 65-74 ,1998.

Kruse, F.A. Boardman, J.W. Lefkoff, A.B. Heidebrecht, K.B. Shapiro, A.T. Barloon P.J. and Goetz, A.F.H.,The Spectral Image Processing System (SIPS) – Interactive Visualization and Analysis of Imaging Spectrometer Data. Rem. Sens. Environ, 44: 145-163 ,1993.

Kujjo, C.P. ,Application of remote sensing for gold exploration in the NubaMontains, Sudan. Bowling Green State University ,Master of Science Thesis , 2010.

Lowell, J.D., Guilbert, J.M., Lateral and vertical alteration mineralization zoning in porphyry ore deposits. Econ. Geol.65, 373–408 ,1997.

Malekzadeh, A..Karimpour , M.H Stern C.R. and Mazaheri, S.A.,Hydrothermal alteration mapping in SW Birjand, Iran , using the Advanced Spaceborne Thermal Emission and Reflection Radiometer (ASTER) image processing. Journal of applied science,s 9 (5): 829-842 ,2009.

Moghtaderi A., Moore F., Mohammadzadeh A., 2007.The application of advanced space-borne thermal emission and reflection (ASTER) radiometer data in the detection of alteration in the Chadormalupaleocrater, Bafq region, Central Iran. Journal of Asian Earth Sciences 30: 238-252.

Papadaki, S. E. Mertikas S. P. and Sarris, A. ,Identification of Lineaments with Possible Structural origin Using ASTER Images and DEM Derive Products in Western Crete, GREECE, European Association of Remote Sensing Laboratories (ARSeL) ,2011.

Raup,B.,Kaab,A.,Kargel,J.,Bishop,M.,Hamilton,G.,Lee,E.,Paul,F.,Rau,F., Soltesz, D., Khalsa, S., 2007. Remote sensing and GIS technology in the Global Land Ice Measurements from Space (GLIMS) Project.Comput.Geosci. 33 (1), 104–125.

Rowan, L.C., Schmidt, R.G., Mars, J.C., 2006. Distribution of hydrothermally altered rocks in the RekoDiq, Pakistan mineralized area based on spectral analysis of ASTER data. Remote Sensing Environ. 104 (1), 74–87.

Rowan L.C., Mars J.C., 2003.Lithologic mapping in the Mountain Pass, California area using Advanced Spaceborne Thermal Emission and Reflection Radiometer (ASTER) data. Remote Sensing of Environment 84, 350-366.

Sabins, F. F., Remote sensing for mineral exploration. Ore Geology Reviews, 14, 157–183, 1999.

Sadeghi, B., Khalajmasoumi, M., Afzal, P., Moarefvand, P., Yasrebi, A. B., Wetherelt, A., Foster, P., Ziazarifi, A., Using ETM+and ASTER sensors to identify iron occurrences in the Esfordi1:100,000 mapping sheet of Central Iran, Journal of African Earth Sciences, 85 (2013) 103–114.

Sarp, G.,Lineament Analysis from Satellite Images, North-West of Ankara, Master of Science Dissertation, School of Natural and Applied Science of Middle East Technical University ,2005.

Watanabe, H., and Matsuo, K., Rock type classification by multi - band TIR of ASTER. Geoscience Journal, 7, 4, 347-358, 2003.

Weldemariam, A. F., Mapping hydrothermally altered rocks and lineament analysis throughdigital enhancement of ASTER data case Study: Kemashi area, Western Ethiopia, Master of Science dissertation, Addis Ababa University, 2009.

Yamaguchi,Y.,Fujisada,H.,Tsu,H.,Sato,I.,Watanabe,H.,Kato,M.,Kudoh,M., Kahlc, A.B., Pnicl, M., 2001. Aster early image evaluation. Adv. Space Res. 28 (1), 69–76.

Yetkin, E. Toprak V. and Suezen, M.L., Alteration Mapping By Remote Sensing: Application toHasandağ -Melendiz Volcanic, Complex. Geo-Imagery Bridging Continents XXth ISPRS Congress, Istanbul, 2004.

Yousefifar S., Khakzad A., AsadiHarooni H., Karami J., Jafari M.R., VosoughiAbedin M., 2011. Prospection of Au and Cu bearing targets by exploration data combination in southern part of Dalli Cu-Au porphyry deposit, Central Iran. Arch. Min. Sci., Vol. 56, No. 1, p. 21-34.

Table 1. The result of PCA for enhancing iron oxide zone

| Eigenvector | B1 | B2 | B3 | B4 |
|---|---|---|---|---|
| PC1 | 0.012737 | 0.015711 | 0.015149 | 0.999681 |
| PC2 | 0.658300 | 0.694763 | -0.289351 | -0.014921 |
| PC3 | -0.064492 | -0.330516 | -0.941376 | 0.020281 |
| PC4 | 0.749880 | -0.638606 | 0.172794 | -0.002137 |

Table 2. The result of PCA for enhancing argillic zone

| Eigenvector | B1 | B4 | B5 | B7 |
|---|---|---|---|---|
| PC1 | 1.000000 | 0.000000 | 0.000000 | -0.000000 |
| PC2 | -0.000000 | 1.000000 | -0.000000 | 0.000000 |
| PC3 | -0.000000 | 0.000000 | 1.000000 | 0.000000 |
| PC4 | 0.000000 | -0.000000 | -0.000000 | 1.000000 |

Table 3. The result of PCA for enhancing phyllic zone

| Eigenvector | B1 | B3 | B5 | B6 |
|---|---|---|---|---|
| PC1 | 1.000000 | 0.000000 | 0.000000 | 0.000000 |
| PC2 | 0.000000 | -1.000000 | 0.000000 | 0.000000 |
| PC3 | -0.000000 | 0.000000 | 1.000000 | - 0.000000 |
| PC4 | 0.000000 | -0.000000 | - 0.000000 | -1.000000 |

Table 4. The result of PCA for enhancing propylitic zone

| Eigenvector | B2 | B5 | B8 | B9 |
|---|---|---|---|---|
| PC1 | 1.000000 | 0.000000 | 0.000000 | 0.000000 |
| PC2 | -0.000000 | 1.000000 | - 0.000000 | - 0.000000 |
| PC3 | -0.000000 | 0.000000 | 1.000000 | -0.000000 |
| PC4 | - 0.000000 | 0.000000 | 0.000000 | 1.000000 |

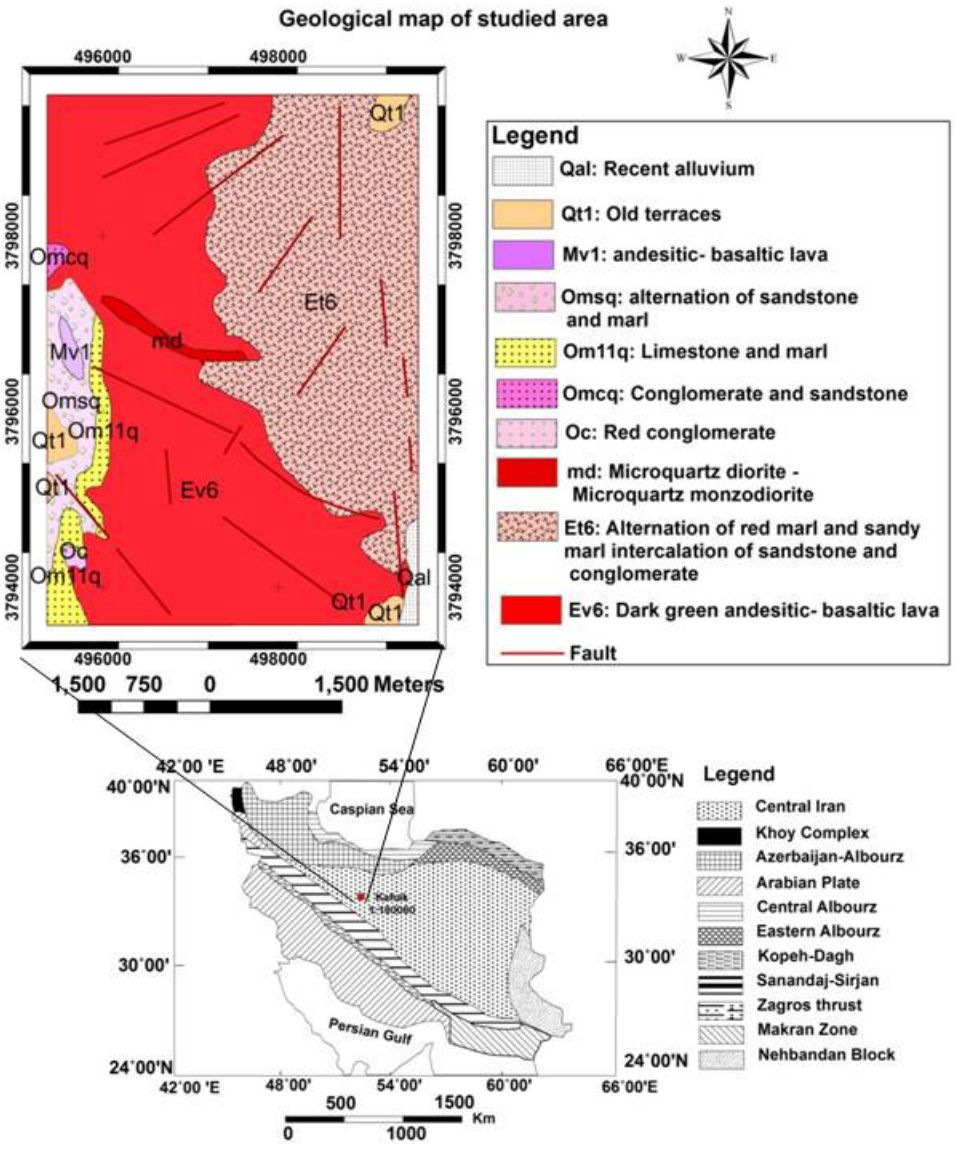


Figure 1. Tectonic map of Iran (Stocklin and Nabavi, 1972)(down), geology map of the Studied area (up).

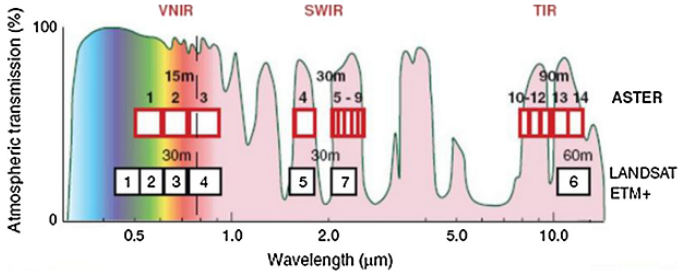


Figure 2. Spectral bands of ASTER and Landsat ETM sensors (Raup et al., 2007).

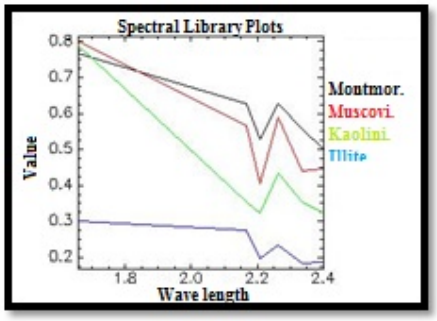


Figure3 .The remarkable mineral reflection for phyllic and argillic zones.

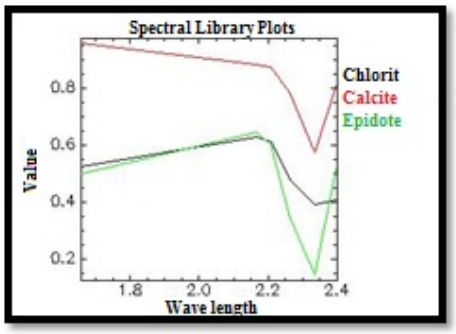


Figure4.The remarkable mineral reflection for propyliticaltration zones.

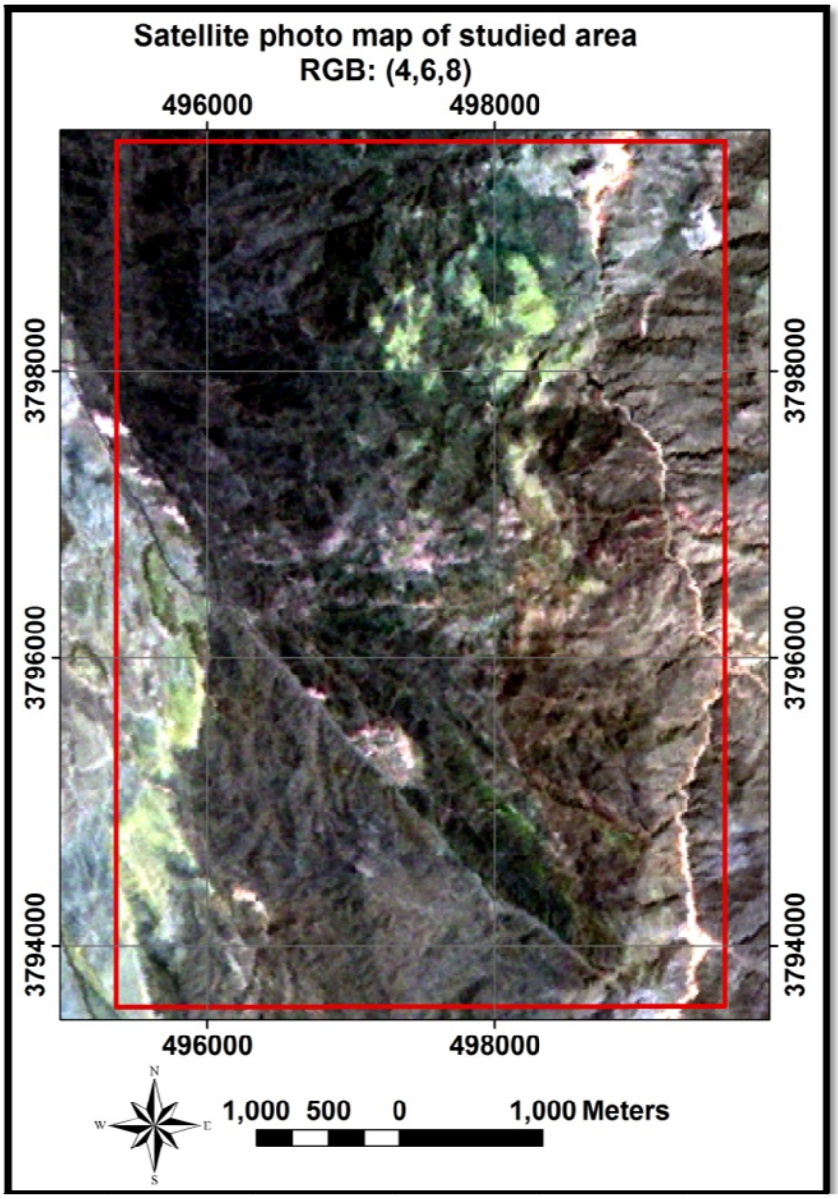


Figure5. RGB (4,6,8): In this color composite, Propylitic alteration appears as green, and Phyllic alteration zones with large quantities of Al-OH minerals are pinkish to yellowish in color. (For interpretation of the references to color in this figure legend, the reader is referred to the web version of this article.).

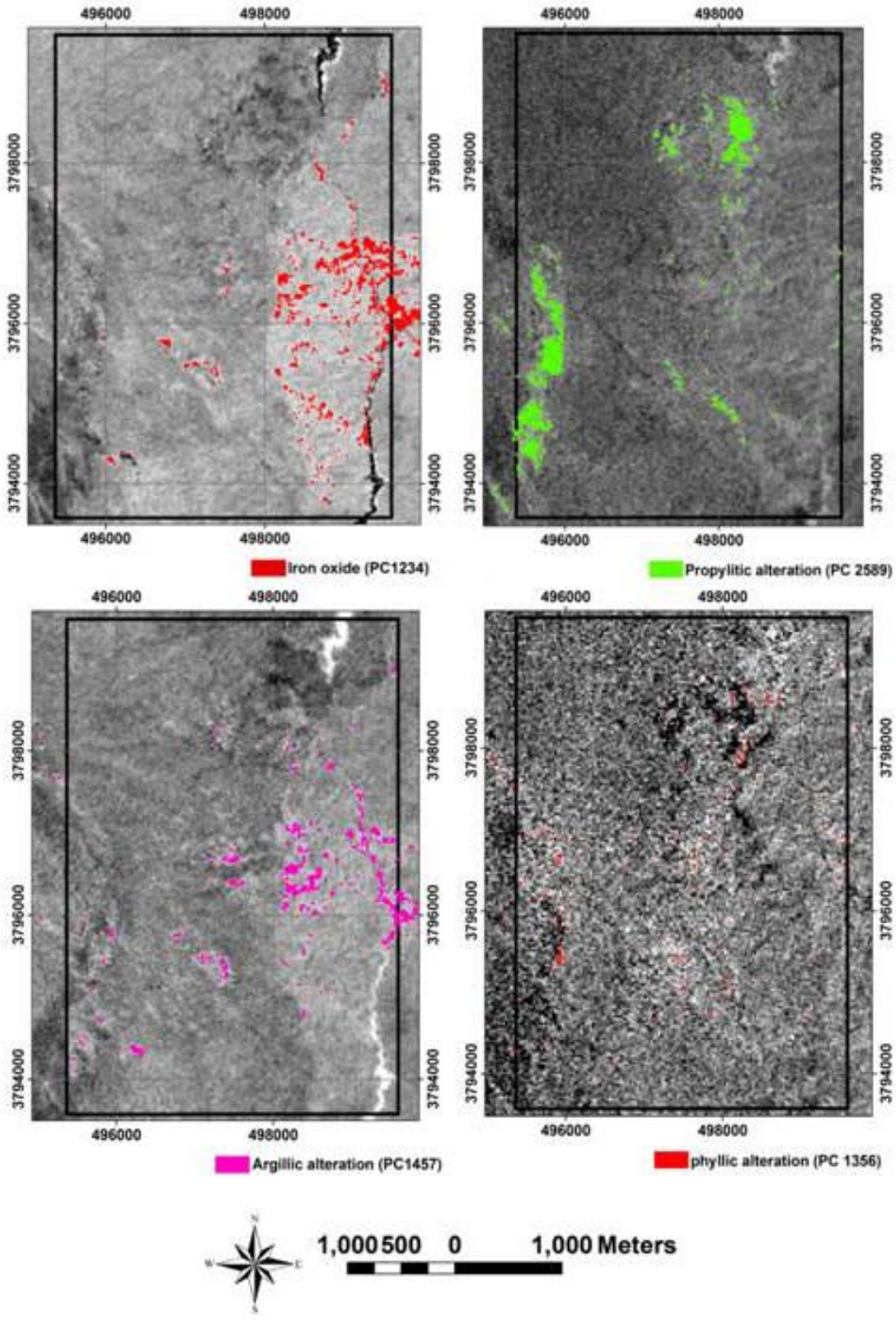


Figure 6.The iron oxide, argillic, phyllic and propylitic images prepared based on PCA method.

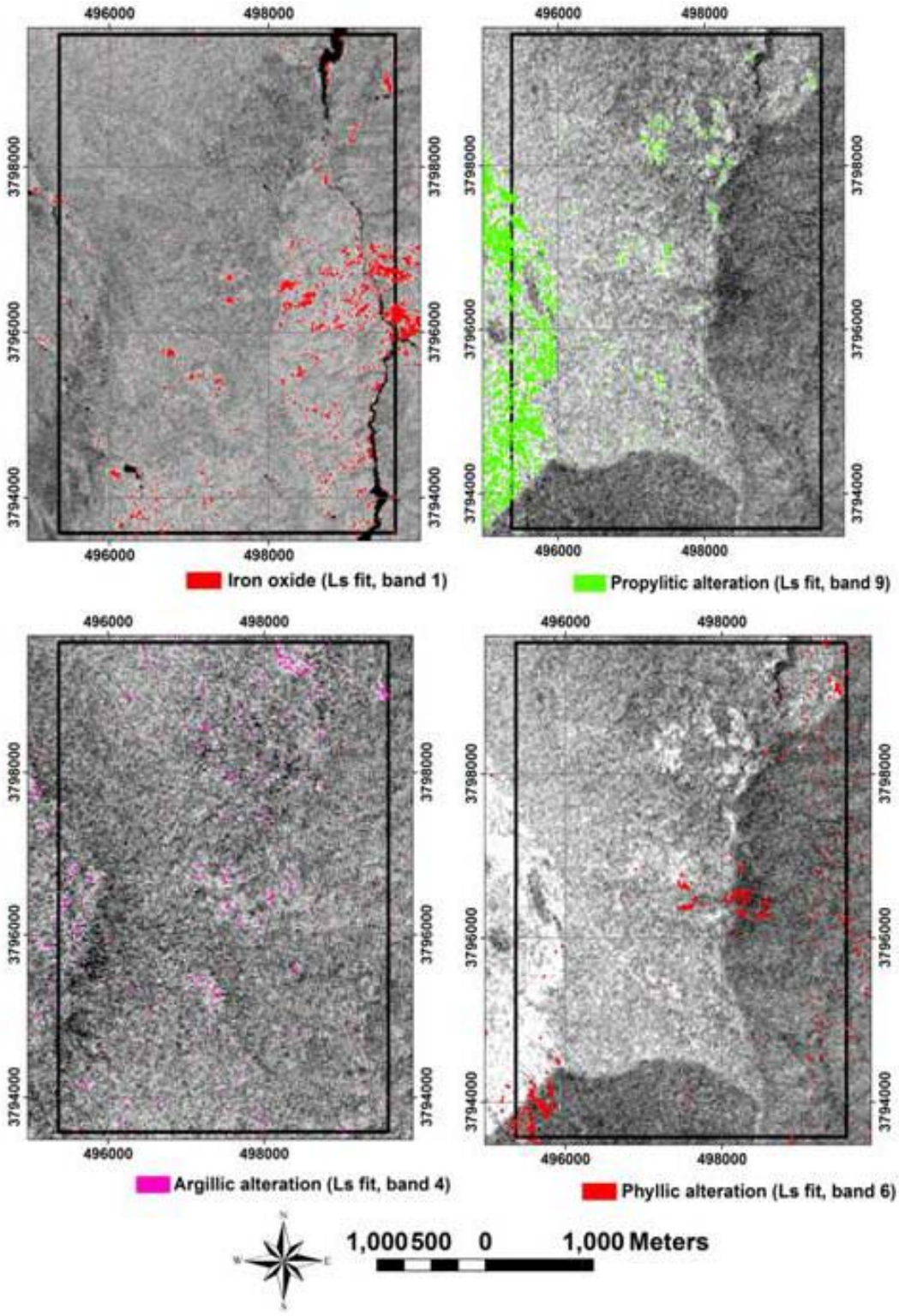


Figure 7.The iron oxide, argillic, phyllic and propylitic images prepared based on LS-Fit method.

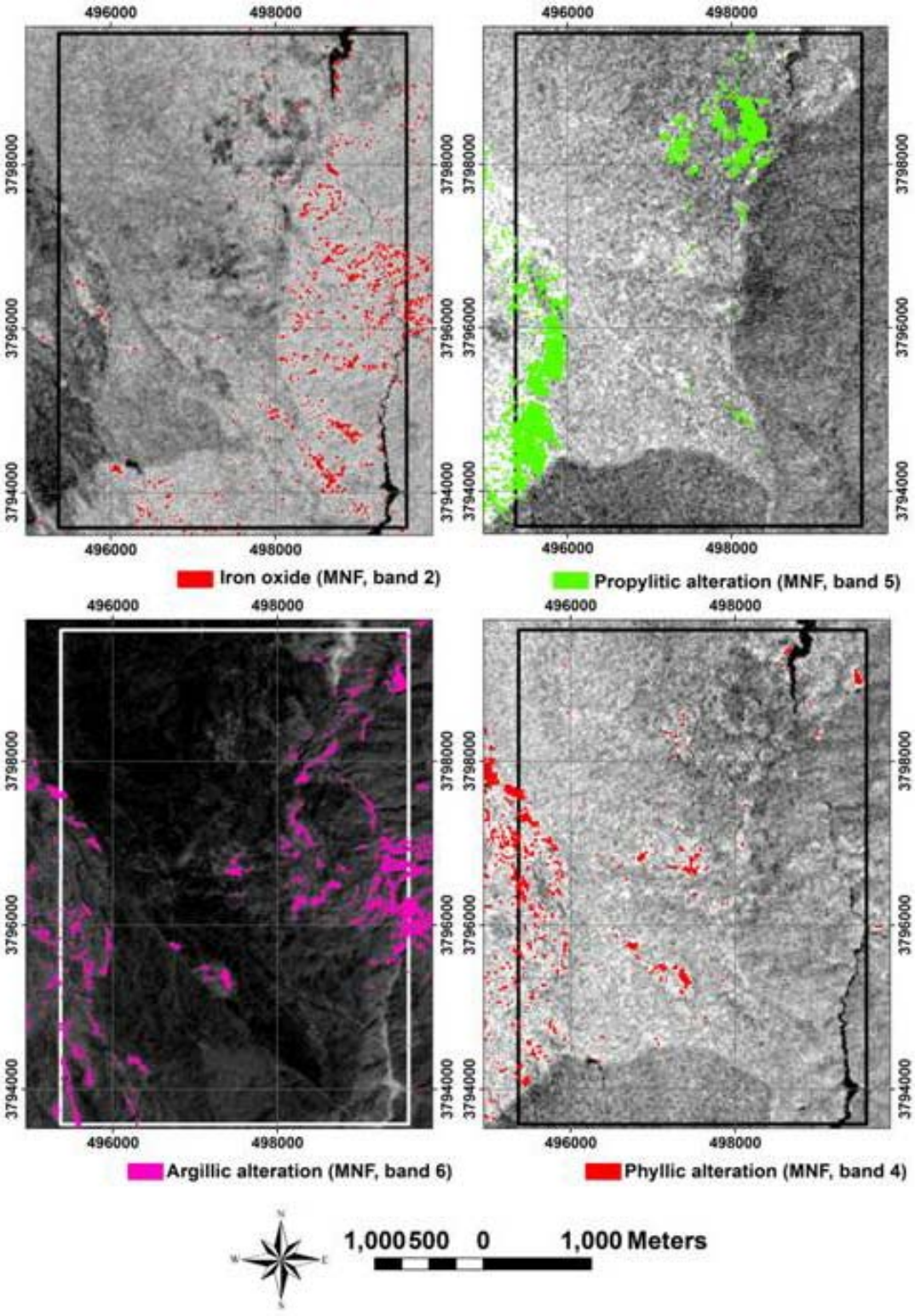


١

٢ Figure 8.The The iron oxide, argillic, phyllic and propylitic images prepared based on MNF

٣ method.

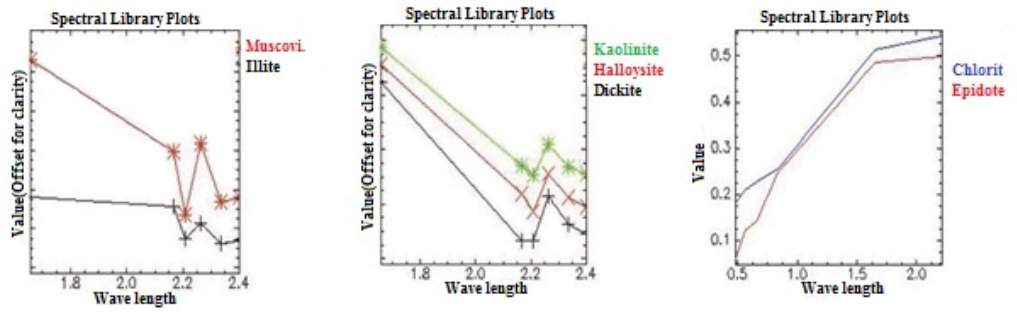


Figure 9.Spectral library plots from USGS library.

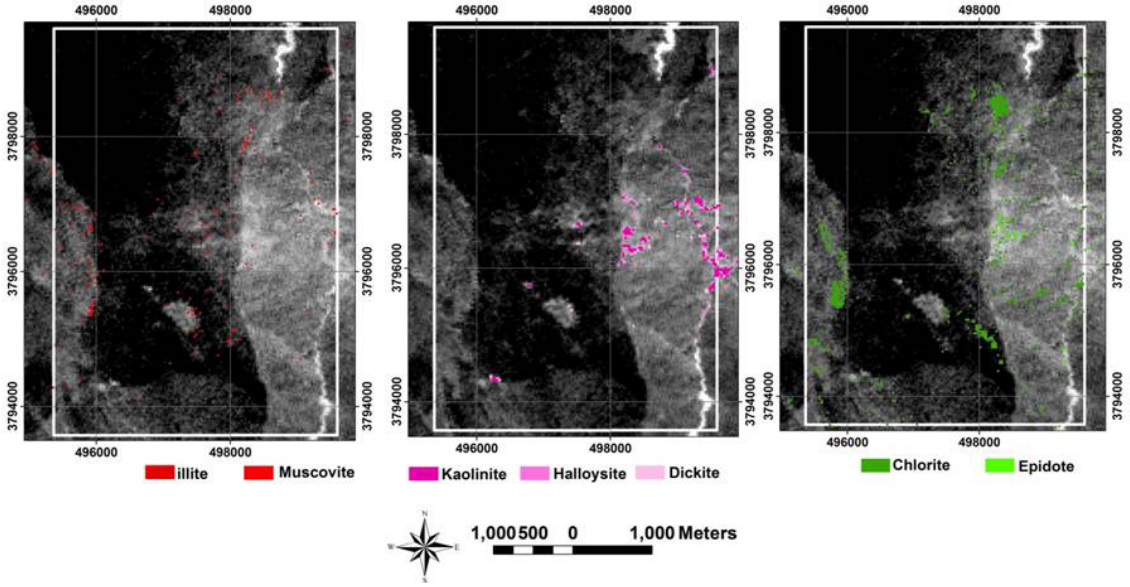


Figure 10.argillic, phyllic, and propylitic images prepared based on SAM method.

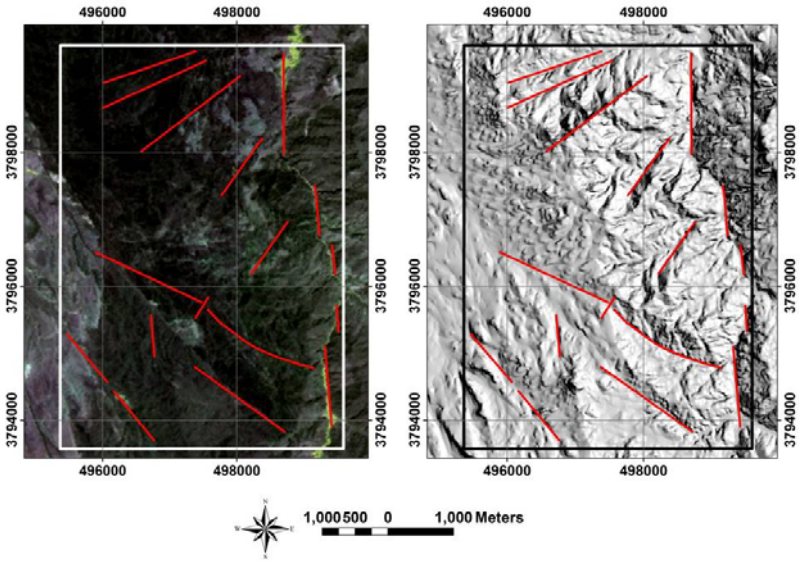


Figure 11.Lineament of studied area based on color composite (left) and shaded relief (right).

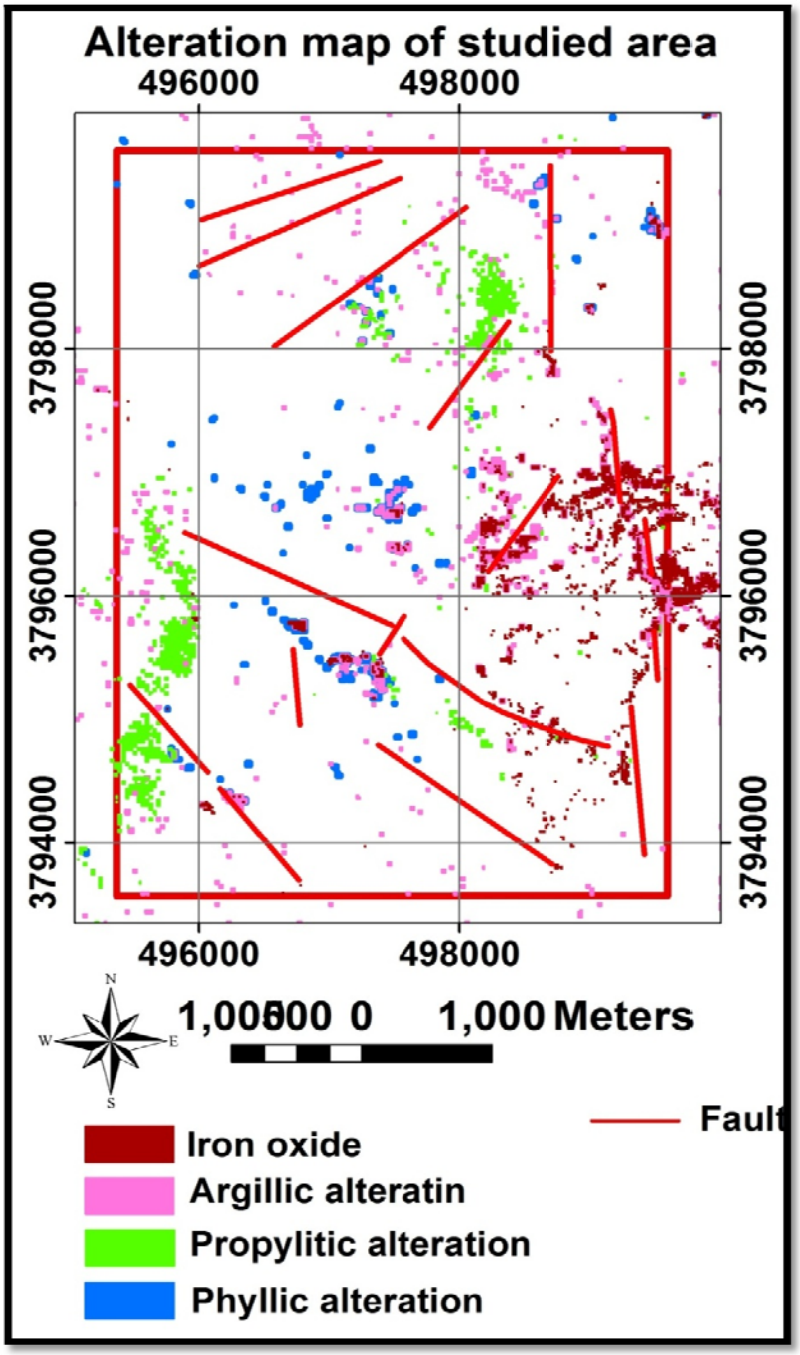


Figure 12.Integration of alteration and lineament.

Figure 13.A full view of studied area.

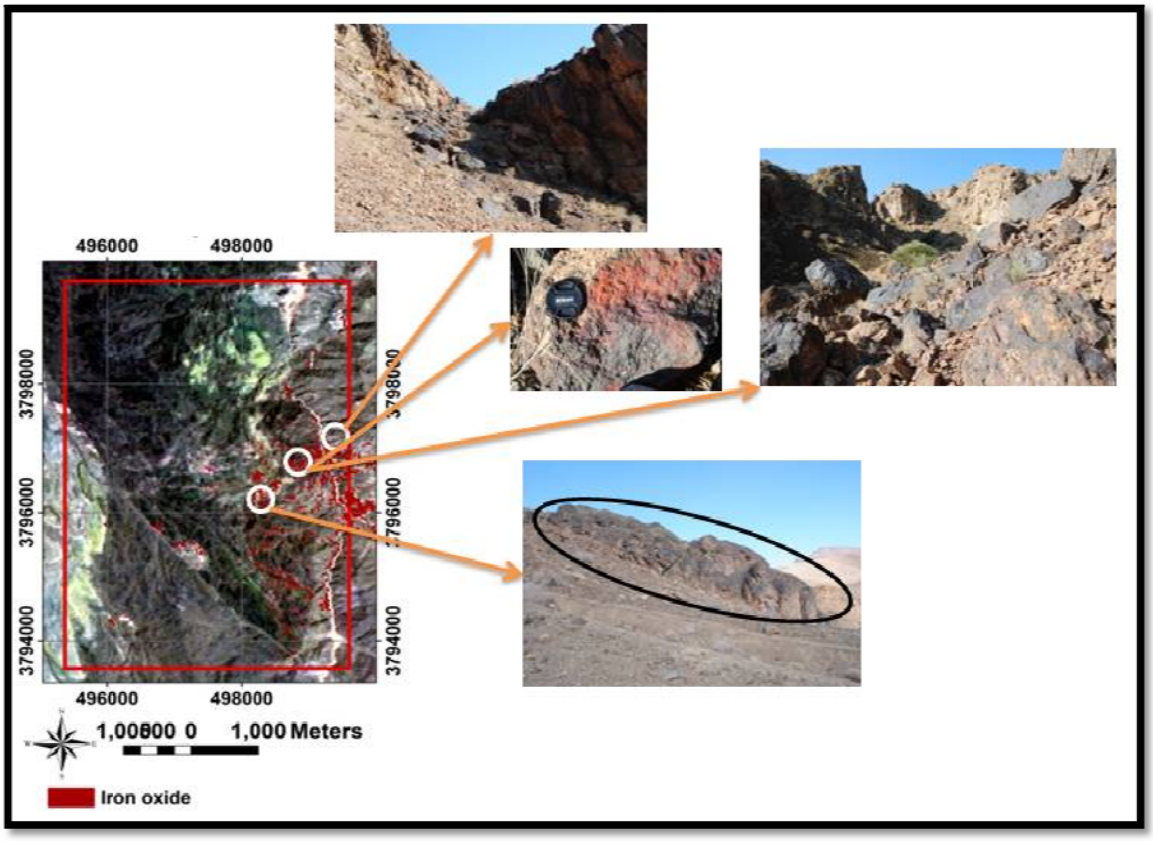


Figure 14.Check field for Iron Oxide zones.

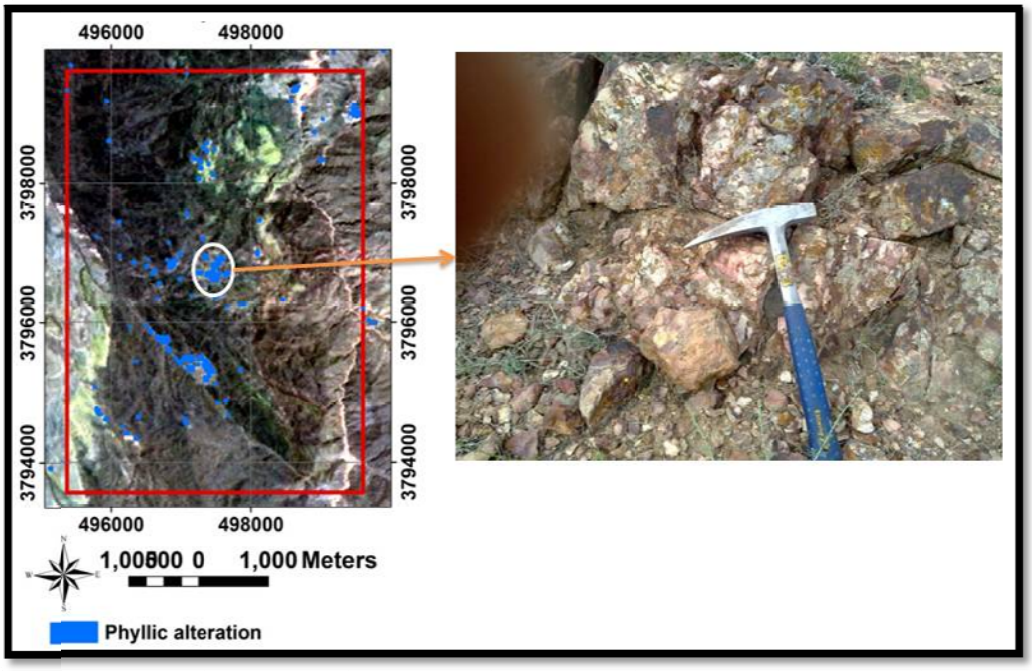


Figure 15.Check field for Phyllic alteration zones.


Figure 16.Check field for Argillic alteration zones.

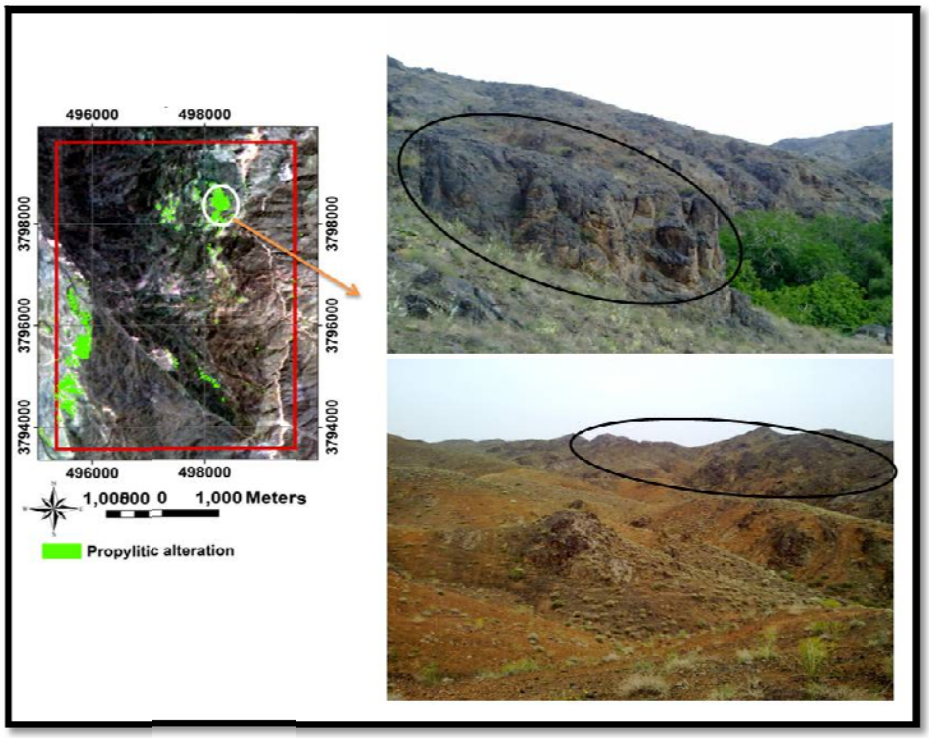


Figure 17.Check field for Propylitic alteration zones.

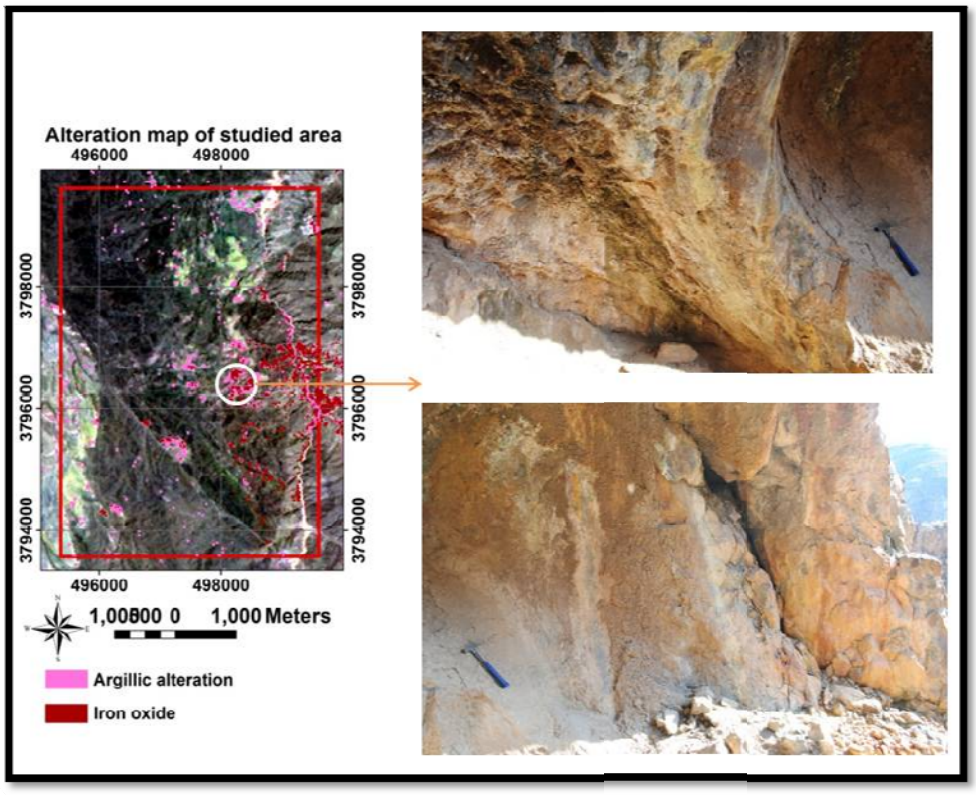


Figure 18.Check field for Hydrothermal alteration zones.

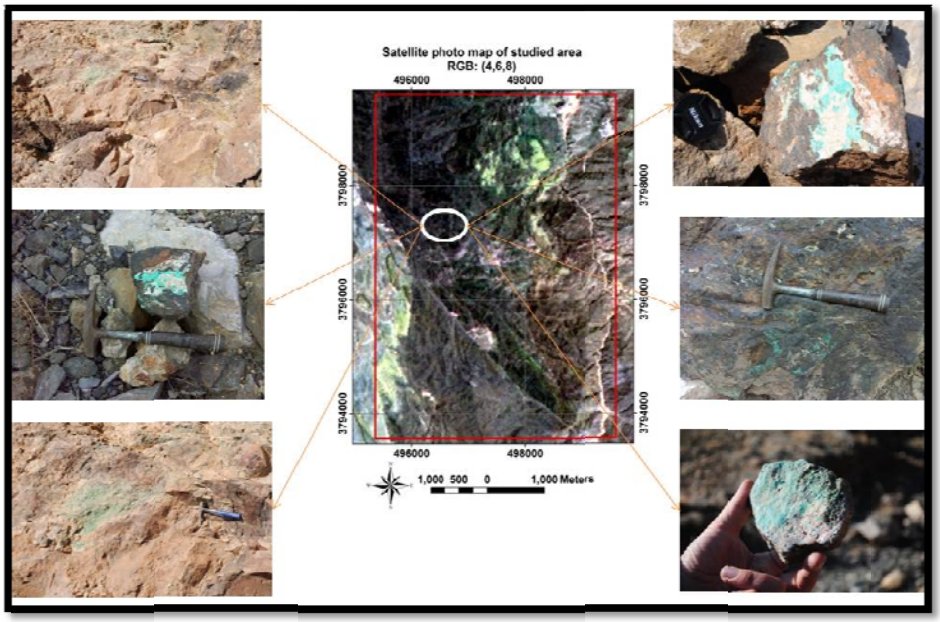


Figure19. Check field for mineralization in porphyry system.